ACS APPLIED MATERIALS & INTERFACES

Research Article

www.acsami.org

Conjugated Polymer Nanoparticles for Fluorescence Imaging and Sensing of Neurotransmitter Dopamine in Living Cells and the Brains of Zebrafish Larvae

Cheng-Gen Qian, Sha Zhu, Pei-Jian Feng, Yu-Lei Chen, Ji-Cheng Yu, Xin Tang, Yun Liu, and Qun-Dong Shen*

Department of Polymer Science & Engineering and Key Laboratory of High Performance Polymer Materials & Technology of MOE, School of Chemistry & Chemical Engineering, Nanjing University, Nanjing 210093, China

Supporting Information

ABSTRACT: Nanoscale materials are now attracting a great deal of attention for biomedical applications. Conjugated polymer nanoparticles have remarkable photophysical properties that make them highly advantageous for biological fluorescence imaging. We report on conjugated polymer nanoparticles with phenylboronic acid tags on the surface for fluorescence detection of neurotransmitter dopamine in both living PC12 cells and brain of zebrafish larvae. The selective enrichment of dopamine and fluorescence signal amplification characteristics of the nanoparticles show rapid and high-sensitive probing such neurotransmitter with the detection limit of 38.8 nM, and minimum interference from other endogenous molecules. It demonstrates the potential of nanomaterials as a multifunctional nanoplatform for targeting, diagnosis, and therapy of dopamine-relative disease.

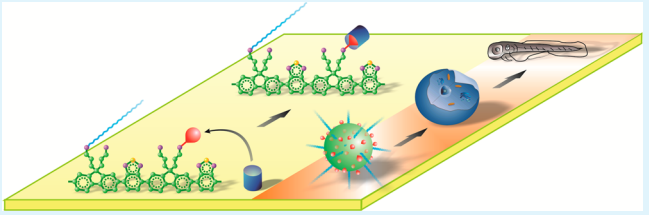

KEYWORDS: *conjugated polymers, nanoparticles, dopamine, fluorescence sensing, bioimaging*

1. INTRODUCTION

Nanoscale materials are attracting a great deal of attention for biological applications that include medical imaging labels, biosensors, delivery of drugs, diagnostics, and therapy of various diseases.[1−6] Conjugated polymer nanoparticles are now being actively investigated in biological optical imaging, *in vivo* tumor targeting, selective recognition of biomolecules, drug carriers, and medical diagnostics/therapeutics.[7−13] They have highly efficient light harvesting and emitting; as a consequence, fluorescence measurements can be carried out in the nanomolar to femtomolar concentration range.[14,15] Other properties of interest include high emission rates, little blinking, minimal dark fraction, and exceptional resistance to photodegradation and chemical degradation, compared to small molecular dyes. The efficient cellular uptake and good biocompatibility make them highly advantageous as labels for biological or medical imaging.[16−20] It is sufficient to detect individual nanoparticles using a visible-light microscope with extremely high spatial resolution. Nanoscale three-dimensional optical tracking has also been demonstrated.[21] It is extraordinarily useful for investigating a wide variety of cellular processes such as molecule transport and membrane dynamics.

Dopamine is a neurotransmitter inside the brain that plays a key role in motivation, reward, habit learning, and motor control. The abnormal dopamine neurotransmission level is correlated to medical conditions such as Parkinson's disease, depression, and drug addiction.[22−24] The increasing interest in dopamine requires facile and reliable sensing techniques, for instance, electrochemical assays and field-effect transistor sensors.[25−28] The great advantages of electrochemical methods are their detection speed and convenience. However, the selectivity is limited for overlap of oxidation potential of dopamine with many other substances (e.g., ascorbic acid) in the central nervous system. The field-effect transistor sensors have very high sensitivity and extremely low detection limits. However, their size scale impedes the application *in vivo*. Because of its high sensitivity and noninvasiveness, fluorescence technique can achieve *in vivo* response of the biomolecules and aptness for living cells and tissues.[29−32] π-Conjugated polymers as fluorescence probes are being actively investigated in biological sensors and imaging.[33−40]

Endogenous dopamine has been found in concentrations of 0.01−1 μM in the brain of bovine, rats, and humans.[41] It is also present with redox active interfering biomolecules, causing considerable difficulties in dopamine analysis. In this paper, we design conjugated polymer nanoparticles for fluorescence imaging and sensing neurotransmitter dopamine in both the living cells and brain of zebrafish larva. The nanoparticles have fluorescence emissive core and phenylboronic acid (PBA) tags on the surface (see Scheme 1). PBA acts as binding sites to dopamine through specific recognition of boronic acid to diol.[42] The nanoparticles with multiple binding sites can selectively

Received: June 5, 2015
Accepted: August 4, 2015
Published: August 4, 2015

DOI: 10.1021/acsami.5b04987
ACS Appl. Mater. Interfaces 2015, 7, 18581−18589

Scheme 1. Sensing Neurotransmitter Dopamine by Conjugated Polymer Nanoparticles[a]

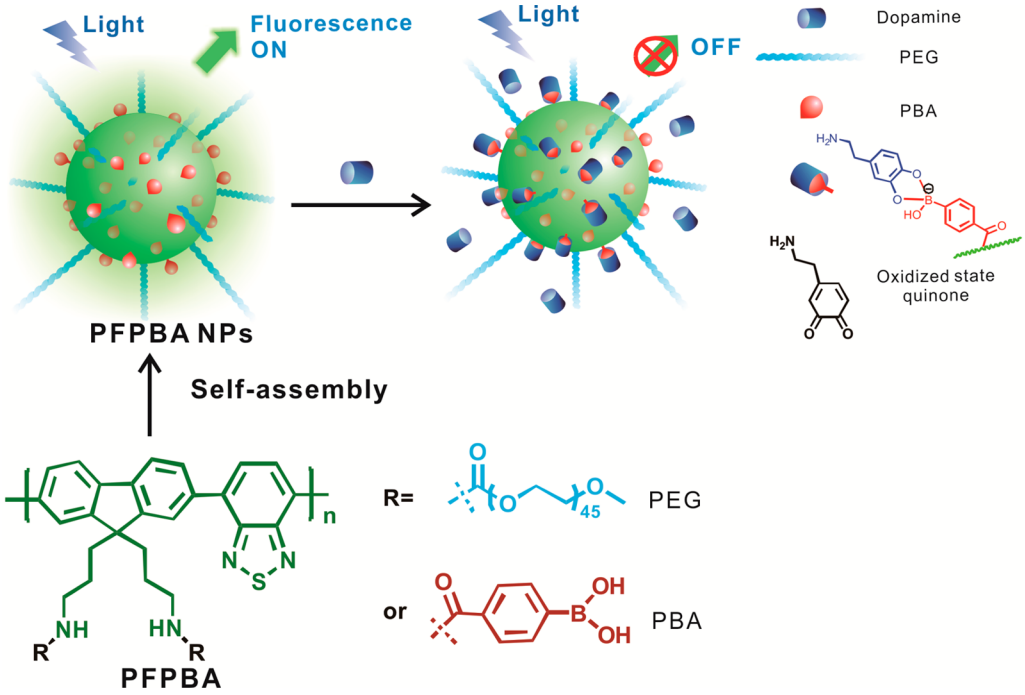

[a]The nanoparticles are obtained by self-assembly of amphiphilic conjugated polymer PFPBA and have phenylboronic acid tags on the surface as binding sites to the dopamine molecules. The binding event results in fluorescence quenching by photo-induced charge transfer between the nanoparticles and dopamine.

extract and enrich dopamine. Dopamine and its oxidation product (quinone) are electron donor and acceptor, respectively; while the nanoparticles under optical excitations can generate bound excitons or free charge carriers and effectively transport electrons along fully conjugated polymer chains. A fast charge transfer between the nanoparticles and dopamine is expected when the charges move to trapping sites of dopamine. Such photoinduced charge transfer (PCT) process will result in fluorescence quenching, reporting the binding event in a very short time. The selective enrichment of dopamine and fluorescence signal amplification characteristics of the conjugated polymer nanoparticles show high-sensitive probing such neurotransmitter. To improve their biodistribution, the nanoparticles are coated with polyethylene glycol (PEG) shells, which are used to enhance their aqueous solubility and colloidal stability, as well as reduce their immunogenic response for *in vivo* applications.

2. EXPERIMENTAL SECTION

2.1. Materials and Instruments. 4,7-Bis(4,4,5,5-tetramethyl-1,3,2-dioxaborolan-2-yl)-2,1,3-ben-zothiadiazole, di-*tert*-butyl dicarbonate (Boc_2O), potassium *tert*-butoxide (BuOK), *N*,*N*′-dicyclohexyl-carbodiimide (DCC), 4-dimethyl-aminopyridine (DMAP), and 4-carboxyphenyl-boronic acid (PBA) were purchased from TCI (Shanghai). Methoxypoly-(ethylene glycol) succinimidyl ester (PEG-SC, average molecule weight of 2000) was purchased from Xiamen Sinopeg Biotech Co., Ltd. (Xiamen, China). Tetrakis(triphenyl-phosphine)-palladium(0) ($Pd(PPh_3)_4$), 2,7-dibromo-fluorene, 3-aminopropyl bromide hydrobromide, dopamine hydrochloride, and other chemicals were purchased from Sigma−Aldrich Co., Ltd. All organic solvents were purchased from Nanjing Chemical Works, and all chemicals were used as received, without further purification, unless otherwise specified. Methylthiazolyl-diphenyl-tetrazolium bromide (MTT) was purchased from Beyotime Institute of Biotechnology (Haimen, China). Annexin V-FITC/PI Cell Apoptosis Kit was obtained from BD Biosciences (USA). Trypsin, penicillin, streptomycin, fetal bovine serum (FBS), and Dulbecco's Modified Eagle Medium (DMEM, high glucose) cell culture medium were purchased from Hyclone (Waltham, USA). Cy5-labeled tyrosine hydroxylase antibodies (TH-anti/Cy5) and PC12 cells were obtained from KeyGen BioTECH (Nanjing, China). Zebrafish was purchased from Nanjing YSY Biotech Company, Ltd. (Nanjing, China).

NMR spectra were measured using a Bruker Model DRX-500 spectrometer. The gel permeation chromatography (GPC) measurement was determined by a Water-410 system with tetrahydrofuran (THF) as the eluent. Particle size distributions and average hydrodynamic diameters were performed on a Malvern Mastersizer 2000 particle size analyzer. The morphologies of the nanoparticles were characterized by transmission electron microscope (JEOL, Model JEM-1011). Ultraviolet−visible (UV-vis) absorption spectra were collected on a Mapada Model UV-1800 spectrophotometer. Fluorescence spectra were measured on Horiba Jobin Yvon Model FM-4NIR spectrophotometer. Confocal laser scanning microscopy (CLSM) was performed in a Zeiss Model LSM710 laser scanning confocal fluorescence microscope. Zebrafish microinjection system was supplied by Nanjing YSY Biotech Company, Ltd. (Nanjing, China).

2.2. Synthesis of PFBT-NH_2. The synthesis routes to poly[9,9-di(3′-aminopropyl)-2,7-fluorenyl-*alt*-4,7-(2,1,3-benzothiadiazole)] (PFBT-NH_2) are shown in Scheme 2. Triethylamine (1.2 mL, 8 mmol) was added to a stirred mixture of 3-aminopropyl bromide hydrobromide (1.75 g, 8 mmol) and 30 mL of CH_2Cl_2 in an ice bath. Di-*tert*-butyl dicarbonate

DOI: 10.1021/acsami.5b04987
ACS Appl. Mater. Interfaces 2015, 7, 18581−18589

Scheme 2. Synthesis Routes to the Conjugated Polymers

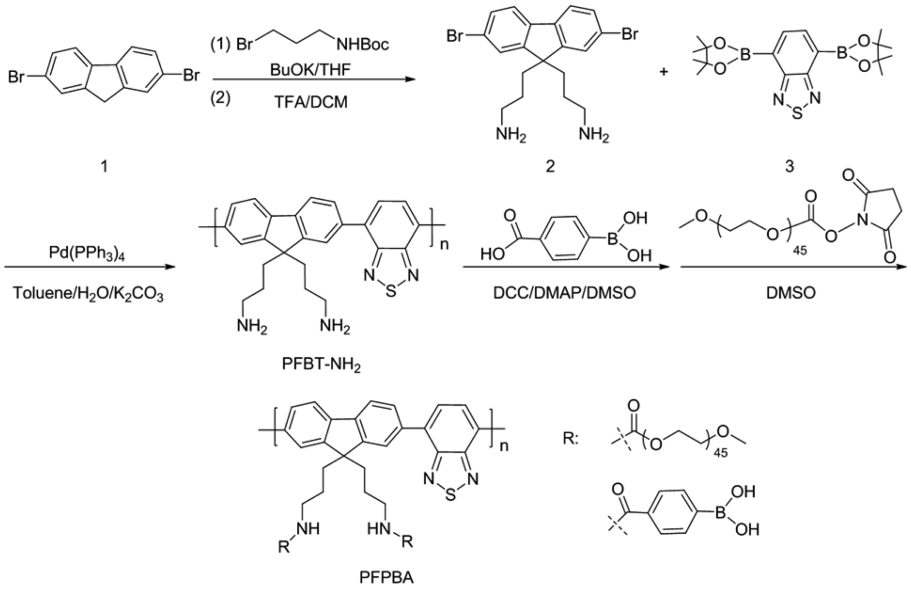

(1.75 g, 8 mmol) in 50 mL of CH_2Cl_2 solution was added dropwise within 10 min. The reaction mixture was stirred at room temperature for 24 h. Ethyl acetate (40 mL) was added, and the reaction mixture was washed with aqueous NaOH (5 wt %), water, and saturated brine (each for three times) and then dried over anhydrous Na_2SO_4. After removal of the solvent, the residue was yellow oil. It was then purified again according to the above method to afford *tert*-butyl-3-bromopropylcarbamate as a pale white solid (1.79 g, 93.9%). ^{1}H NMR (500 MHz, $CDCl_3$, δ): 1.45 (s, 9H), 2.05 (m, 2H), 3.28 (m, 2H), 3.44 (t, 2H), 4.66 (s, 1H).

A mixture of 2,7-dibromofluorene (1.83 g, 5.65 mmol), *tert*-butyl-3-bromopropylcarbamate (3.36 g, 14.1 mmol), and THF (15 mL) was carefully degassed and charged with argon. Degassed potassium *tert*-butoxide (1.43 g, 12.7 mmol) in THF solution (50 mL) was added into the mixture in a dropwise manner. The reaction mixture was stirred at room temperature for 48 h. After the removal of the solvent, the residue was dissolved in 50 mL of CH_2Cl_2 and washed with aqueous NaOH (5 wt %), water, and saturated brine (each for three times) and then dried over anhydrous Na_2SO_4. After the removal of the solvent, the residue was purified by chromatography on silica gel column eluting with ethyl acetate/ligroin (v:v, 1:6) to afford 2,7-dibromo-9,9-bis(3-*tert*-butyl propylcarbamate) fluorene as a pale white solid (2.65 g, 73.4%). ^{1}H NMR (500 MHz, $CDCl_3$, δ): 0.75 (m, 4H), 1.39 (s, 18H), 1.95 (t, 4H), 2.89 (s, 4H), 4.25 (s, 2H), 7.43 (s, 2H), 7.47 (d, 2H), 7.52 (d, 2H).

TFA (3 mL) was added to a solution of 2,7-dibromo-9,9-bis(3-*tert*-butylpropyl-carbamate) fluorene (0.75 g, 1.18 mmol) in CH_2Cl_2 (5.5 mL). The mixture was stirred at room temperature for 2 h. After the addition of hydrochloric acid, the mixture was extracted with CH_2Cl_2. Aqueous NaOH was added to the water phase, and the mixture was then placed in a refrigerator overnight. A large amount of white precipitates were formed, via filtration and evaporation, to afford 2,7-dibromo-9,9-bis(3-aminopropyl) fluorene (**2**) as a white solid (0.49 g, 94.9%). ^{1}H NMR (500 MHz, DMSO-d_6, δ): 0.54 (m, 4H), 1.25 (s, 4H), 1.99 (m, 4H), 2.25 (t, 4H), 7.53 (d, 2H), 7.69 (s, 2H), 7.80 (d, 2H).

2,7-Dibromo-9,9-bis(3-aminopropyl) fluorene (**2**) (0.22 g, 0.5 mmol), 4,7-bis(4,4,5,5-tetramethyl-1,3,2-dioxaborolan-2-yl)-2,1,3-benzothiadiazole (**3**) (0.19 g, 0.5 mmol), and $Pd(PPh_3)_4$ (50 mg) were dissolved in a degassed mixture of toluene (25 mL) and K_2CO_3 aqueous solution (2 mol/L, 12.5 mL). The mixture was stirred at 85−90 °C for 2 days under an argon atmosphere. After cooling to room temperature, the mixture was extracted with chloroform, washed with brine and distilled water, and then precipitated from acetone to afford a yellow solid with 37% yield. ^{1}H NMR (500 MHz, $CDCl_3$, δ): 0.9−1.0 (m, $-CCH_2C-$), 2.0 (m, $-CH_2-$fluorene), 2.2−2.5 (m, $-CH_2-$N), 7.4−7.7 (m, fluorene ring), 7.9−8.0 (m, aromatic rings). The molecular weight of PFBT-NH_2 was determined by GPC (calibrated by polystyrene standard). The weight-average molecular weight of PFBT-NH_2 was 11 000 g/mol, and the polydispersity was 1.21.

2.3. Synthesis of PFPBA. PFBT-NH_2 was allowed to react with 4-carboxyphenylboronic acid and methoxypoly(ethylene glycol) succinimidyl ester, coupling their carboxyl groups with the amino group of the polymer (Scheme 2). Briefly, PFBT-NH_2 (0.12 mmol) and DMAP (0.04 mmol) were added in anhydrous DMSO (20 mL) solution containing PBA (0.15 mmol) and DCC (0.15 mmol) in an ice bath with argon. The mixture was stirred for 1 h at 0 °C, and then 24 h at room temperature. Then, PEG-SC (0.09 mmol) was added and stirred for 3 days at room temperature. After being placed in a refrigerator overnight, the precipitate, 1,3-dicyclohexylurea (DCU), was filtered off and the filtrate was dialyzed against distilled water for 3 days using a membrane with a cutoff molecular weight of 8000−10 000 g/mol. The resulting aqueous solution was then freeze-dried and the product was vacuum-dried overnight to yield PFPBA. ^{1}H NMR (500 MHz, DMSO-d_6, δ): 1.7 (m, $-CCH_2C-$), 2.0 (m, $-CH_2-$fluorene), 3.4−3.6 (m, $CH_3-O-CH_2-CH_2-O$, $-CH_2-N-$), 6.7 (s, $-NH-CO$), 7.2−7.7 (m, fluorene ring), 8.0−8.2 (m, aromatic rings). ^{11}B NMR (160.4 MHz, DMSO-d_6, δ): 26.9.

2.4. Preparation of PFPBA Nanoparticles. The nanoparticles of the polymer PFPBA were prepared by a solvent-exchange method.[43] Briefly, PFPBA (5 mg) was dissolved in THF (2 mL) and stirred for 3 h at room temperature.

DOI: 10.1021/acsami.5b04987
ACS Appl. Mater. Interfaces 2015, 7, 18581−18589

Distilled water (4 mL) was added to the THF solution by syringe with stirring (850 rpm) at speed of 2 mL/h. The mixture solution was dialyzed against distilled water for 24 h, using a membrane with a cutoff molecular weight of 8000−10000 g/mol. The PFPBA nanoparticle suspension was filtered through a 0.45 μm microfilter, and then stored at 4 °C.

2.5. Fluorescence Detection of Dopamine by PFPBA Nanoparticles. The fluorescence spectrum of 10 μM PFPBA nanoparticles in PBS buffer (20 mM, pH 7.40) was collected 10 times to determine the background noise σ. The solution then was treated with dopamine of concentrations from 0.025−10 μM, and all spectra were collected after mixing for 30 min. The slope of the curve of emission intensity ratio $(I_0 - I)/I_0$ of the nanoparticles and logarithmic value of dopamine concentration was obtained using simple linear regression. The detection limit (3σ/slope) was then determined.

2.6. Cell Culture and Confocal Fluorescence Imaging of Dopamine. The PC12 cells were seeded in confocal microscope dishes at an intensity of 1×10^5/mL in DMEM supplemented with 10% FBS and 1% penicillin/streptomycin, and cultured for 24 h at 37 °C in a humidified atmosphere containing 5% CO_2. The cells were incubated with 10 μM PFPBA nanoparticles at 37 °C for 2 h, and then washed by PBS twice, followed by incubation with Cy5-labeled tyrosine hydroxylase antibodies (TH-anti/Cy5) for 2 h. Subsequently, the cells were divided into two groups: one incubated with fresh PBS for 30 min and the other was treated with anaerobic PBS[27] (anaerobic buffer was prepared by continuously bubbling PBS buffer, sealed in a clean glass flask, with pure N_2 gas (purity: 5N) through a steel needle for 15 min. Subsequently, P (O_2) reduced buffers were prepared by volume-to-volume mixing the aerobic and anaerobic buffers). The images of the cells were collected by a confocal laser scanning microscope (Zeiss, Model LSM 710). PFPBA NPs signals were collected at 505−600 nm with an excitation wavelength of 488 nm (laser power = 5.5%), and tyrosine hydroxylase signals were collected at 640−710 nm with an excitation wavelength of 633 nm (laser power = 8.0%).

2.7. Cytotoxicity Analysis. MTT assay was exploited to determine the cytotoxicity of PFPBA nanoparticles. The cells were seeded in a 96-well plate at the intensity of 0.5×10^4 cells per well in DMEM containing 10% FBS and 1% penicillin/streptomycin at 37 °C in a humidified atmosphere containing 5% CO_2 for 24 h. The medium then was replaced by DMEM supplemented with PFPBA nanoparticles with different concentrations for 24 h. After that, the DMEM culture with the nanoparticles was replaced with PBS, and 10 μL of MTT (0.5 mg/mL) solution was added to each well and incubated for 4 h. The supernatant then was removed and the products were lysed with 200 μL of DMSO. The absorbance values were recorded at 580 nm using a microplate reader (Thermo Electron Corporation). The absorbance of the untreated cells was used as a positive control and its absorbance was set as the reference value for calculating 100% cellular viability.

2.8. Apoptosis Assay. Apoptosis of PC12 cells was detected using Annexin V-FITC Apoptosis Detection Kit. The cells (1×10^5 cells per well) were seeded in six-well plates. After culture for 48 h, the cells were incubated with PFPBA nanoparticles with different concentrations for 12 h. The subsequent procedures were performed in accordance with the manufacturer's protocol. The cells then were analyzed by flow cytometry (Beckman Coulter CytoFLEX).

2.9. *In Vivo* Observation of PFPBA Nanoparticles for Dopamine Sensing in the Brain of Zebrafish Larvae. Zebrafish embryos or larvae were incubated in pure water at 28.5 °C. Zebrafish larvae were microinjected with PFPBA nanoparticles (10 μM) or a mixture of the nanoparticles (10 μM) and dopamine (1 μM), respectively. Afterward, zebrafish larvae embedded in methyl cellulose were imaged, respectively, usign a laser scanning confocal fluorescence microscope with 10× and 20× objectives at an excitation wavelength of 405 nm.

3. RESULTS AND DISCUSSION

3.1. Preparation and Characterization of PFPBA Nanoparticles. The nanoparticles are fabricated from self-assembly of PFPBA (Scheme 1). The fluorescent core of the nanoparticles is a hydrophobic π-conjugated polymer; i.e., they are alternative copolymers of fluorene and benzothiadiazole (PFBT-NH_2), where fluorenes alone are high-efficient blue-emitting materials and benzothiadiazole is effective in shifting emission maximum of the conjugated polymer to longer wavelengths. PFBT-NH_2 is then modified by PBA and PEG (molar ratio = 5:3). The desired PBA groups are introduced by the reaction of primary amine groups on side chains of the conjugated polymer with 4-carboxy-phenylboronic acid in the presence of *N*,*N*′-dicyclohexyl-carbodiimide (DCC) and 4-dimethylaminopyridine. It leads to an electron-withdrawing amide carbonyl on the phenylboronic acid moiety that reduces the pK_a value of boronic acid monomer, which responds to dopamine at physiological pH. Consequently, the flexible hydrophilic PEG chains are introduced by reaction of methoxypoly(ethylene glycol) succinimidyl ester (average molecule weight of 2000) with other primary amines present on the conjugated polymer. Only one signal is observed in ^{11}B NMR spectrum of PFPBA, where the chemical shift is 26.9 ppm and characteristic of trigonal boronic acid. Characteristic peaks corresponding to the protons in methylene of the repeat unit of PEG side chains is found at 3.4−3.6 ppm in the ^{1}H NMR spectrum of PFPBA. The ratio of PBA group and the PEG group was calculated from ^{1}H NMR to be 2/1.

PFPBA nanoparticles are obtained through the solvent-exchange method, wherein the polymer is initially dissolved in tetrahydrofuran, and then distilled water is slowly added via syringe under stirring. Absorption and fluorescence emission spectra of PFPBA nanoparticles in aqueous suspension are shown in Figure 1A. The nanoparticles has two absorption bands, at 309 and 419 nm, which arise from the light absorption by the π-electron system of the conjugated backbone, and an emission maximum at 529 nm with a Stokes shift of ∼110 nm. Benzothiadiazole units in polymer main chains lead to a significant red-shift of the excitation wavelength, with respect to that of polyfluorene. Thus, the conjugated nanoparticles hold great potential for further fluorescence sensing or tracking in living cells using blue light excitation to minimize ultraviolet-induced photodamage.

The dynamic light scattering (DLS) measurement shows that the nanoparticles in aqueous suspension have a unimodal size distribution with average hydrodynamic diameter of 120 nm (Figure 1B). The morphology of the conjugated polymer nanoparticles is observed using transmission electron microscopy (inset of Figure 1B). The spherical shape of the nanoparticles is clearly distinguished with a diameter slightly smaller than that in aqueous suspension, because of the collapse of outermost PEG layers during the drying process and observation in the high vacuum environment. Water is a good

DOI: 10.1021/acsami.5b04987
ACS Appl. Mater. Interfaces 2015, 7, 18581−18589

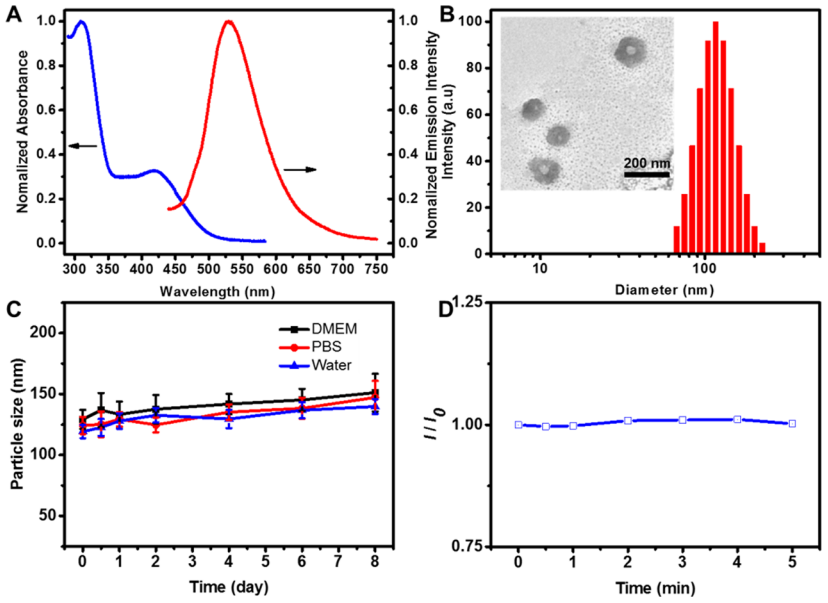

Figure 1. (A) Normalized UV-vis absorption and emission spectra of PFPBA nanoparticles in aqueous suspension. The excitation wavelength is 410 nm. (B) Hydrodynamic diameter distribution and TEM image (inset) of the nanoparticles. (C) Average size changes of PFPBA nanoparticles incubated in water, PBS buffer (pH 7.4), or DMEM for 8 days. (D) Photostability of PFPBA nanoparticles upon irradiation under ultraviolet light (60 W).

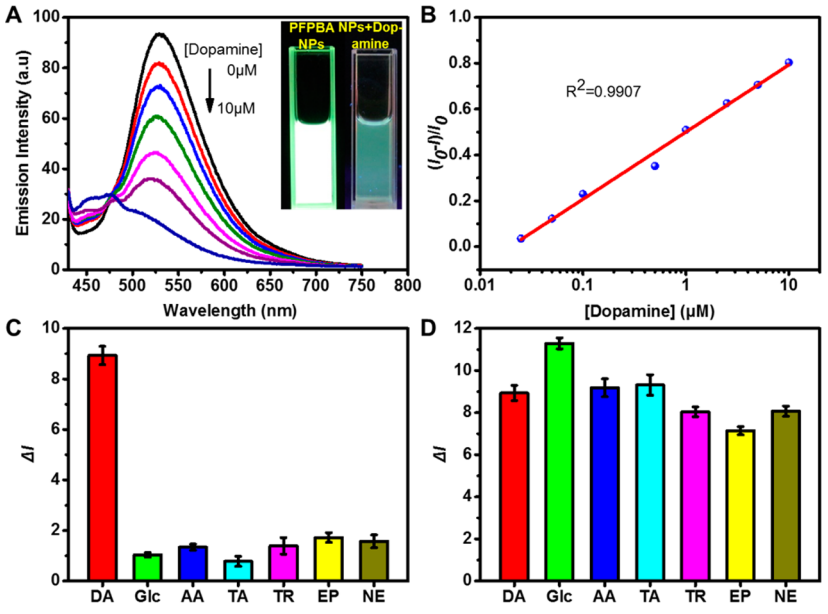

Figure 2. (A) Fluorescence spectra of PFPBA nanoparticles (10 μM) in PBS (20 mM, pH 7.4) obtained upon titration with dopamine from 0 to 10 μM. The excitation wavelength is 410 nm. Inset: photographs show the nanoparticles (10 μM) in PBS buffer and their response to dopamine (1 μM). (B) The emission intensity ratio $[(I_0 - I)/I_0]$ of the nanoparticles in PBS buffer (20 mM, pH 7.4), as a function of logarithmic concentration of dopamine. (C, D) The emission intensity change (ΔI) of PFPBA nanoparticles (10 μM) in PBS buffer (20 mM, pH 7.40) in the presence of (C) dopamine (DA) (0.1 μM), glucose (Glc) (1 μM), ascorbic acid (AA) (1 μM), tyramine (TA) (1 μM), tyrosine (TR) (1 μM), epinephrine (EP) (0.1 μM), norepinephrine (NE) (0.1 μM), and (D) both DA (0.1 μM) and other physiological substances.

solvent for the grafted PEG chains, while the rigid π-conjugated backbones are insoluble in it. Thus, the amphiphilic copolymer tends to form robust, nanoscale, and spherical micelles in the aqueous solution. The expected structure of such micelle-like aggregates after solvent evaporation is an inner conjugated polymer core surrounded by the PEG shell, which is consistent with the observation by the electron microscope.

To evaluate their colloidal stability, pegylated PFPBA nanoparticles are incubated in water, phosphate-buffered saline (PBS, pH 7.4), or Dulbecco's Modified Eagle Medium (DMEM). The average size of the nanoparticles increases only slightly with incubation time, as shown in Figure 1C, and no precipitations are observed even after incubation for 8 days. Figure 1D shows that the fluorescence intensity of PFPBA nanoparticles is very stable upon continuous irradiation by ultraviolet light (60 W) for 5 min. High photostability of the nanoparticles is beneficial for imaging and sensing purposes.

DOI: 10.1021/acsami.5b04987
ACS Appl. Mater. Interfaces 2015, 7, 18581−18589

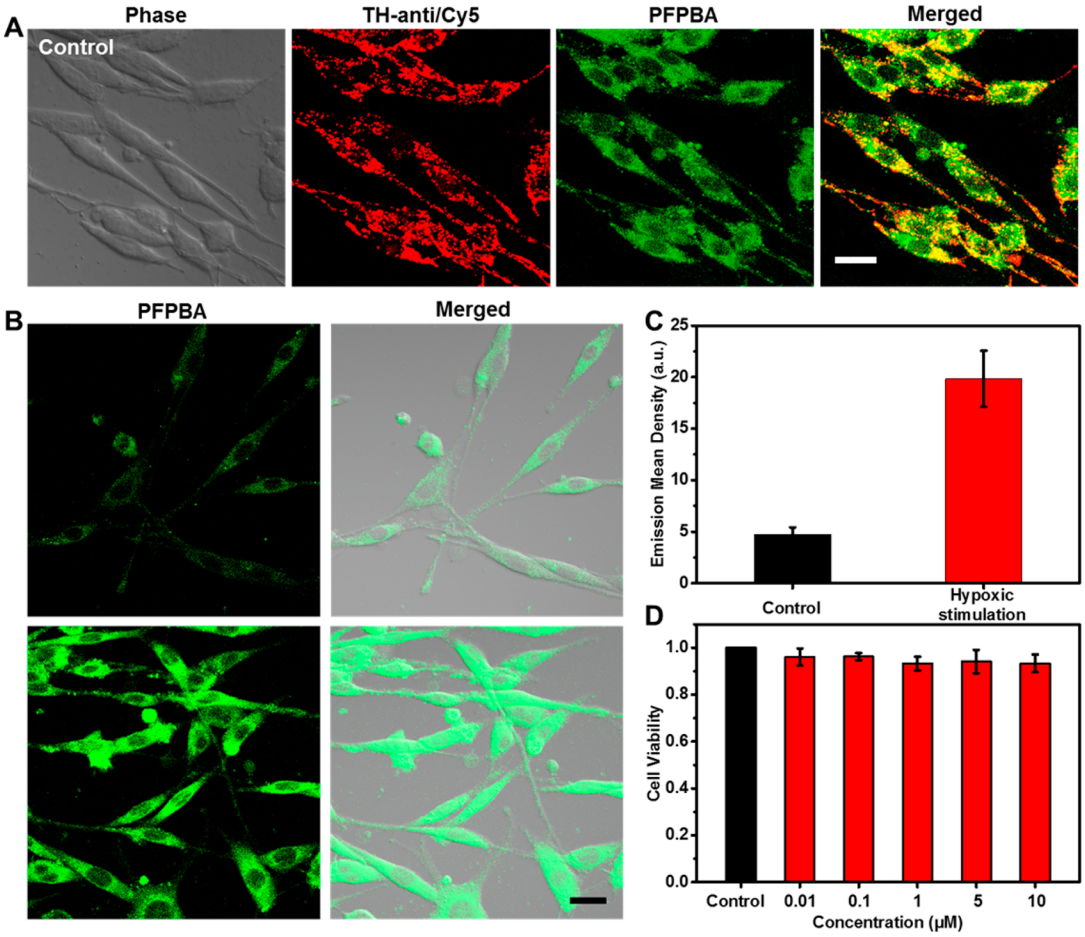

Figure 3. Fluorescence imaging and sensing dopamine by PFPBA nanoparticles in PC12 cells. (A) Co-localization images of PFPBA nanoparticles in PC12 cells. The cells were incubated with 10 μM PFPBA nanoparticles and Cy5-labeled tyrosine hydroxylase antibodies (TH-anti/Cy5) for 2 h, respectively. (Scale bar = 20 μm.) (B) Real-time fluorescence images of PC12 cells that are seeded with PFPBA nanoparticles in response to hypoxic stimulation. The cells were incubated with 10 μM PFPBA nanoparticles for 2 h in normal or 50% P (O_2) reduced hypoxic buffer. (Scale bar = 20 μm.) (C) Emission mean density of the PFPBA nanoparticles in PC12 cells with or without hypoxic stimulation. (D) Cell viability treated with PFPBA nanoparticles on PC12 cells at various concentrations for 24 h.

3.2. *In Vitro* Dopamine Fluorescent Sensing by PFPBA Nanoparticles. Fluorescence sensing behavior of the conjugated polymer nanoparticles with phenylboronic acid tags as dopamine nanoprobes is investigated under physiological conditions. As shown in Figure 2A, the emission intensity at 529 nm from PFPBA nanoparticles (10 μM) in PBS (20 mM, pH 7.4) decreases distinctly. The solution turns from bright green to very pale blue-green under a UV lamp (inset of Figure 2A), suggesting that dopamine molecules can be detected with the naked eye. PFPBA nanoparticles with dopamine are evaluated by the DLS measurements and TEM images (see Figure S1 in the Supporting Information), and no significant change was observed.

As shown in Figure 2B, a good linear relationship is found between the emission intensity ratio $(I_0 - I)/I_0$ of PFPBA nanoparticles and logarithmic concentration of dopamine in the range of 0.025−10 μM (where I_0 and I represent the fluorescence intensity maximum in the absence and presence of dopamine, respectively). The detection limit according to the fluorescence sensing is determined as 38.8 nM. Endogenous dopamine concentrations are in the range of 0.01−1 μM.[41] Thus, PFPBA nanoparticles have great potential for dopamine sensing *in vitro* and *in vivo*. Phenylboronic acid tags on the surface of the nanoparticles act as binding sites to dopamine and form a stable borate ester. The dopamine-triggered fluorescence quenching occurs via a photoinduced charge-transfer process between the nanoparticles and dopamine or its oxidation product quinone. Each nanoparticle contains many PBA groups and can enrich dopamine molecules surrounding it, which increases the chance of fluorescence quenching and realizing high-sensitivity probing in applications such as neurotransmitters.

In vitro or *in vivo* dopamine determination can be interfered with other endogenous substances, including glucose (Glc, typical monosaccharide with 1,2-diol group), ascorbic acid (AA, a major interfering molecule present in cells with a redox potential close to dopamine), tyramine (TA, a structural analogue to dopamine), tyrosine (TR, a biomolecule involved in the dopamine metabolism), and epinephrine/norepinephrine (EP/NE, two other catecholamines). We test the sensing selectivity of PFPBA nanoparticles in PBS buffer (pH 7.4). As can be seen in Figure 2C, a dramatic change in fluorescence signal of the PFPBA nanoparticles is observed for dopamine (DA) with a concentration of 0.1 μM, which is within the physiologically relevant concentration range. Other physiological components (0.1 or 1 μM) only trigger small fluorescence changes. The possibility of specific detection of dopamine in the presence of other endogenous substances is also studied (Figure 2D). The variation in the fluorescence signal intensity of

DOI: 10.1021/acsami.5b04987
ACS Appl. Mater. Interfaces 2015, 7, 18581−18589

PFPBA nanoparticles in the absence or presence of other physiological substances is not remarkable. The high selectivity of the nanoparticles can be ascribed to specific recognition of PBA groups to dopamine. It enhances the accessibility of dopamine quencher to the fluorophores, i.e., the conjugated polymer, and results in much higher fluorescence quenching efficiency than other redox-active species.

3.3. Fluorescence Imaging and Sensing Dopamine by PFPBA Nanoparticles in Living PC12 Cells. PC12 cells are chosen as a dopaminergic neurons cell model to study the intracellular performance of the PFPBA nanoparticles imaging and sensing endogenous dopamine. To identify the intracellular location of PFPBA nanoparticles, the PFPBA nanoparticles-loaded PC12 cells were co-stained with Cy5-labeled tyrosine hydroxylase antibodies (TH-anti/Cy5), respectively. As shown in Figure 3A, after coincubation with TH-anti/Cy5 and PFPBA NPs for 2 h at 37 °C, the Cy5-labeled tyrosine hydroxylase antibodies was located in the neuronal cell bodies and dendrites with point-shaped distribution (red), and PFPBA nanoparticle fluorescence signals shown a bright densely punctuated pattern in the cytoplasm (green). Of note, the PFPBA fluorescence signals could coincide with tyrosine hydroxylase signals in the neuronal cell bodies and dendrites (yellow), indicating directly PFPBA NPs could be easily transported into the cells and detect dopamine inside cells. PFPBA nanoparticles have phenylboronic acid tags on surface that can adhere to glycans or sialic acids on the cell membrane,[41,42] and then undergo internalization after surface binding. The cellular uptake of the nanoparticles is possibly mediated by clathrin-mediated endocytosis, macropinocytosis, or passive diffusion.[20]

PC12 cells can release endogenous dopamine under a hypoxic or Ca^{2+} stimulation.[27,44] Herein, fluorescence images of PFPBA nanoparticles in the living PC12 cells under a hypoxic stimulation are collected by a confocal laser scanning microscope. As shown in Figure 3B, compared with the control groups, the fluorescence from intracellular PFPBA significantly increase in hypoxic condition, indicating that the PFPBA nanoparticles with phenylboronic acid tags were used for real-time fluorescence imaging and sensing endogenous neurotransmitter dopamine in living PC12 cells. The emission mean density of the nanoparticles in the cells is 4-fold of the original value after such natural stimulation, demonstrating exocytosis or release of dopamine (Figure 3C).

As a candidate for biological application, biocompatibility of PFPBA nanoparticles should be evaluated. *In vitro* cell viability determined by MTT colorimetric assay (Figure 3D) and Annexin V-FITC/propidium iodide (PI) assay (see Figure S2 in the Supporting Information). PFPBA nanoparticles presented no significant cytotoxicity within the concentration used in this study. Previous studies show that conjugated polymer nanoparticles are biocompatibility, and thus have great potential for drug delivery, diagnostic, and imaging purposes. In our case, surface coating PEG layers on the nanoparticles can also reduce cytotoxicity.

3.4. Fluorescence Imaging of PFPBA Nanoparticles in Brain of Zebrafish Larva. Zebrafish larvae are then chosen as a model for *in vivo* optical imaging by microinjection of PFPBA nanoparticles (10 μM) into brain ventricles. They are then embedded in methyl cellulose for fluorescence imaging by confocal laser scanning microscopy. The micrographs are taken under light and fluorescent illumination and superimposed. The injected larvae survive, again confirming low toxicity of the PFPBA nanoparticles. Comparison of injected and noninjected

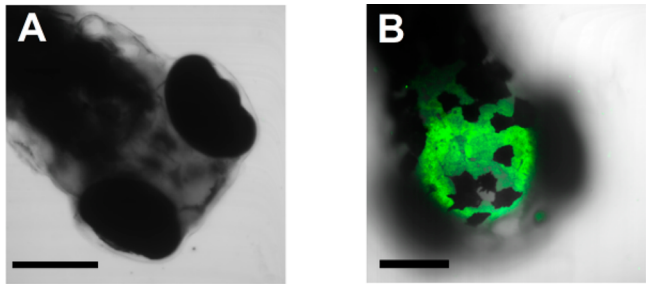

Figure 4. Live imaging of zebrafish brain by confocal laser scanning microscopy: (A) dorsal view before microinjecting fluorescent PFPBA nanoparticles into the brain ventricle and (B) after microinjecting fluorescent PFPBA nanoparticles into the brain ventricle. All images were collected with a band path of 500−650 nm upon irradiation at 405 nm. (Scale bar = 200 μm.)

brains (Figure 4) shows the prominent fluorescence signal from PFPBA nanoparticles in the ventricle, implying that the nanoparticle can be utilized for analyzing brain morphogenesis.

Attempt to observe response of PFPBA nanoparticles to endogenous dopamine is not prone at this stage, partly due to the lack of initial fluorescence intensity. As a complementary approach, when exposed to exogenous dopamine, the brain ventricle with the microinjected nanoparticles shows a significant change of the fluorescence images (Figure 5A). The

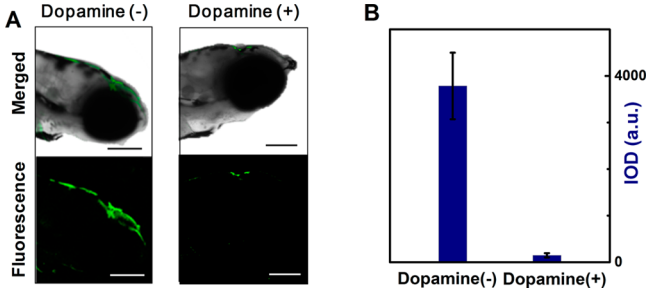

Figure 5. (A) Optical images of zebrafish brain (lateral views) with microinjected PFPBA nanoparticles in the ventricle, in the absence (left) and presence (right) of exogenous dopamine molecules. (B) Integrated optical density (IOD) in the brain ventricles. (Scale bar = 200 μm.)

fluorescence analysis reveals 96% decrease in the integrated optical density (IOD) in the presence of dopamine (Figure 5B), which is consistent with the *in vitro* results.

4. CONCLUSIONS

In summary, we have developed fluorescent nanoparticles with phenylboronic acid tags on the surface for the fluorescence imaging and sensing of neurotransmitter dopamine in living cells and tissues. The high sensitivity and selectivity and good biocompatibility, as well as high photostability, of the conjugated polymer nanoparticles render this formulation as a promising strategy for the detection of neurotransmitters under physiological conditions or inside living cells/tissues. The conjugated polymer nanoparticles can achieve diverse luminescence colors and, in some cases, afford near-infrared emission for deep tissue penetration. Taking into account their large interior cargo volume and their ability to enrich the dopamine molecules surrounding it, the nanoparticles have potential as a multifunctional platform for the diagnosis and therapy of diseases correlated to such neurotransmitters in the future.

DOI: 10.1021/acsami.5b04987
ACS Appl. Mater. Interfaces 2015, 7, 18581−18589

■ ASSOCIATED CONTENT

Supporting Information

The Supporting Information is available free of charge on the ACS Publications website at DOI: 10.1021/acsami.5b04987.

Hydrodynamic diameter distribution and TEM image of PFPBA nanoparticles with dopamine, and flow cytometric analysis of PC12 cell apoptosis induced by PFPBA nanoparticles (PDF)

■ AUTHOR INFORMATION

Corresponding Author

*Tel.: +86-25-8331 7807. Fax: +86-25-8331 7761. E-mail: qdshen@nju.edu.cn.

Notes

The authors declare no competing financial interest.

■ ACKNOWLEDGMENTS

This work was supported by National Natural Science Foundation of China (No. 21174060), Program for Changjiang Scholars and Innovative Research Team in University (No. IRT1252), and China Equipment and Education Resources System (No. CERS-1-45).

■ REFERENCES

(1) Weissleder, R.; Nahrendorf, M.; Pittet, M. J. Imaging Macrophages with Nanoparticles. *Nat. Mater.* **2014**, *13*, 125−138.

(2) Yang, W.; Ratinac, K. R.; Ringer, S. P.; Thordarson, P.; Gooding, J. J.; Braet, F. Carbon Nanomaterials in Biosensors: Should You Use Nanotubes or Graphene? *Angew. Chem., Int. Ed.* **2010**, *49*, 2114−2138.

(3) Kanasty, R.; Dorkin, J. R.; Vegas, A.; Anderson, D. Delivery Materials for Sirna Therapeutics. *Nat. Mater.* **2013**, *12*, 967−977.

(4) Petros, R. A.; DeSimone, J. M. Strategies in the Design of Nanoparticles for Therapeutic Applications. *Nat. Rev. Drug Discovery* **2010**, *9*, 615−627.

(5) Giljohann, D. A.; Seferos, D. S.; Daniel, W. L.; Massich, M. D.; Patel, P. C.; Mirkin, C. A. Gold Nanoparticles for Biology and Medicine. *Angew. Chem., Int. Ed.* **2010**, *49*, 3280−3294.

(6) Gu, Z.; Aimetti, A. A.; Wang, Q.; Dang, T. T.; Zhang, Y.; Veiseh, O.; Cheng, H.; Langer, R. S.; Anderson, D. G. Injectable Nano-Network for Glucose-Mediated Insulin Delivery. *ACS Nano* **2013**, *7*, 4194−4201.

(7) Pecher, J.; Mecking, S. Nanoparticles of Conjugated Polymers. *Chem. Rev.* **2010**, *110*, 6260−6279.

(8) Li, K.; Liu, B. Polymer-Encapsulated Organic Nanoparticles for Fluorescence and Photoacoustic Imaging. *Chem. Soc. Rev.* **2014**, *43*, 6570−6597.

(9) Feng, L.; Zhu, C.; Yuan, H.; Liu, L.; Lv, F.; Wang, S. Conjugated Polymer Nanoparticles: Preparation, Properties, Functionalization and Biological Applications. *Chem. Soc. Rev.* **2013**, *42*, 6620−6633.

(10) Koner, A. L.; Krndija, D.; Hou, Q.; Sherratt, D. J.; Howarth, M. Hydroxy-Terminated Conjugated Polymer Nanoparticles Have Near-Unity Bright Fraction and Reveal Cholesterol-Dependence of Igf1r Nanodomains. *ACS Nano* **2013**, *7*, 1137−1144.

(11) Ahmed, E.; Morton, S. W.; Hammond, P. T.; Swager, T. M. Fluorescent Multiblock Π-Conjugated Polymer Nanoparticles for *In Vivo* Tumor Targeting. *Adv. Mater.* **2013**, *25*, 4504−4510.

(12) Yuan, Y.; Liu, J.; Liu, B. Conjugated-Polyelectrolyte-Based Polyprodrug: Targeted and Image-Guided Photodynamic and Chemotherapy with On-Demand Drug Release Upon Irradiation with a Single Light Source. *Angew. Chem., Int. Ed.* **2014**, *53*, 7163−7168.

(13) Yuan, H. X.; Liu, Z.; Liu, L. B.; Lv, F. T.; Wang, Y. L.; Wang, S. Cationic Conjugated Polymers for Discrimination of Microbial Pathogens. *Adv. Mater.* **2014**, *26*, 4333−4338.

(14) Brouard, D.; Viger, M. L.; Bracamonte, A. G.; Boudreau, D. Label-Free Biosensing Based on Multilayer Fluorescent Nanocomposites and a Cationic Polymeric Transducer. *ACS Nano* **2011**, *5*, 1888−1896.

(15) McQuade, D. T.; Pullen, A. E.; Swager, T. M. Conjugated Polymer-Based Chemical Sensors. *Chem. Rev.* **2000**, *100*, 2537−2574.

(16) Zhu, C.; Liu, L.; Yang, Q.; Lv, F.; Wang, S. Water-Soluble Conjugated Polymers for Imaging, Diagnosis, and Therapy. *Chem. Rev.* **2012**, *112*, 4687−4735.

(17) Wu, C.; Bull, B.; Szymanski, C.; Christensen, K.; McNeill, J. Multicolor Conjugated Polymer Dots for Biological Fluorescence Imaging. *ACS Nano* **2008**, *2*, 2415−2423.

(18) Sun, B.; Sun, M. J.; Gu, Z.; Shen, Q. D.; Jiang, S. J.; Xu, Y.; Wang, Y. Conjugated Polymer Fluorescence Probe for Intracellular Imaging of Magnetic Nanoparticles. *Macromolecules* **2010**, *43*, 10348−10354.

(19) Pu, K.-Y.; Liu, B. Fluorescent Conjugated Polyelectrolytes for Bioimaging. *Adv. Funct. Mater.* **2011**, *21*, 3408−3423.

(20) Liu, Y.; Huang, J.; Sun, M.-J.; Yu, J.-C.; Chen, Y.-L.; Zhang, Y.-Q.; Jiang, S.-J.; Shen, Q.-D. A Fluorescence-Raman Dual-Imaging Platform Based on Complexes of Conjugated Polymers and Carbon Nanotubes. *Nanoscale* **2014**, *6*, 1480−1489.

(21) Yu, J.; Wu, C.; Sahu, S. P.; Fernando, L. P.; Szymanski, C.; McNeill, J. Nanoscale 3d Tracking with Conjugated Polymer Nanoparticles. *J. Am. Chem. Soc.* **2009**, *131*, 18410−18414.

(22) Kim, J. H.; Auerbach, J. M.; Rodríguez-Gómez, J. A.; Velasco, I.; Gavin, D.; Lumelsky, N.; Lee, S.-H.; Nguyen, J.; Sánchez-Pernaute, R.; Bankiewicz, K.; McKay, R. Dopamine Neurons Derived from Embryonic Stem Cells Function in an Animal Model of Parkinson's Disease. *Nature* **2002**, *418*, 50−56.

(23) Chaudhury, D.; Walsh, J. J.; Friedman, A. K.; Juarez, B.; Ku, S. M.; Koo, J. W.; Ferguson, D.; Tsai, H. C.; Pomeranz, L.; Christoffel, D. J.; Nectow, A. R.; Ekstrand, M.; Domingos, A.; Mazei-Robison, M. S.; Mouzon, E.; Lobo, M. K.; Neve, R. L.; Friedman, J. M.; Russo, S. J.; Deisseroth, K.; Nestler, E. J.; Han, M. H. Rapid Regulation of Depression-Related Behaviours by Control of Midbrain Dopamine Neurons. *Nature* **2013**, *493*, 532−536.

(24) Volkow, N. D.; Fowler, J. S.; Wang, G.-J.; Swanson, J. M. Dopamine in Drug Abuse and Addiction: Results from Imaging Studies and Treatment Implications. *Mol. Psychiatry* **2004**, *9*, 557−569.

(25) Yue, H. Y.; Huang, S.; Chang, J.; Heo, C.; Yao, F.; Adhikari, S.; Gunes, F.; Liu, L. C.; Lee, T. H.; Oh, E. S.; Li, B.; Zhang, J. J.; Huy, T. Q.; Luan, N. V.; Lee, Y. H. Zno Nanowire Arrays on 3d Hierachical Graphene Foam: Biomarker Detection of Parkinson's Disease. *ACS Nano* **2014**, *8*, 1639−1646.

(26) Schmidt, A. C.; Wang, X.; Zhu, Y.; Sombers, L. A. Carbon Nanotube Yarn Electrodes for Enhanced Detection of Neurotransmitter Dynamics in Live Brain Tissue. *ACS Nano* **2013**, *7*, 7864−7873.

(27) Li, B.-R.; Hsieh, Y.-J.; Chen, Y.-X.; Chung, Y.-T.; Pan, C.-Y.; Chen, Y.-T. An Ultrasensitive Nanowire-Transistor Biosensor for Detecting Dopamine Release from Living Pc12 Cells under Hypoxic Stimulation. *J. Am. Chem. Soc.* **2013**, *135*, 16034−16037.

(28) Zhang, M.; Liao, C.; Yao, Y.; Liu, Z.; Gong, F.; Yan, F. High-Performance Dopamine Sensors Based on Whole-Graphene Solution-Gated Transistors. *Adv. Funct. Mater.* **2014**, *24*, 978−985.

(29) Rodriguez, P. C.; Pereira, D. B.; Borgkvist, A.; Wong, M. Y.; Barnard, C.; Sonders, M. S.; Zhang, H.; Sames, D.; Sulzer, D. Fluorescent Dopamine Tracer Resolves Individual Dopaminergic Synapses and Their Activity in the Brain. *Proc. Natl. Acad. Sci. U. S. A.* **2013**, *110*, 870−875.

(30) Pradhan, T.; Jung, H. S.; Jang, J. H.; Kim, T. W.; Kang, C.; Kim, J. S. Chemical Sensing of Neurotransmitters. *Chem. Soc. Rev.* **2014**, *43*, 4684−4713.

(31) Kruss, S.; Landry, M. P.; Vander Ende, E.; Lima, B. M.; Reuel, N. F.; Zhang, J.; Nelson, J.; Mu, B.; Hilmer, A.; Strano, M. Neurotransmitter Detection Using Corona Phase Molecular Recognition on Fluorescent Single-Walled Carbon Nanotube Sensors. *J. Am. Chem. Soc.* **2014**, *136*, 713−724.

DOI: 10.1021/acsami.5b04987
ACS Appl. Mater. Interfaces 2015, 7, 18581−18589

(32) Jeon, S.-J.; Kwak, S.-Y.; Yim, D.; Ju, J.-M.; Kim, J.-H. Chemically-Modulated Photoluminescence of Graphene Oxide for Selective Detection of Neurotransmitter by "Turn-on" Response. *J. Am. Chem. Soc.* **2014**, *136*, 10842−10845.
(33) Pinto, M. R.; Schanze, K. S. Amplified Fluorescence Sensing of Protease Activity with Conjugated Polyelectrolytes. *Proc. Natl. Acad. Sci. U. S. A.* **2004**, *101*, 7505−7510.
(34) Jiang, H.; Taranekar, P.; Reynolds, J. R.; Schanze, K. S. Conjugated Polyelectrolytes: Synthesis, Photophysics, and Applications. *Angew. Chem., Int. Ed.* **2009**, *48*, 4300−4316.
(35) Feng, X. L.; Liu, L. B.; Wang, S.; Zhu, D. B. Water-Soluble Fluorescent Conjugated Polymers and Their Interactions with Biomacromolecules for Sensitive Biosensors. *Chem. Soc. Rev.* **2010**, *39*, 2411−2419.
(36) Dmitriev, R. I.; Borisov, S. M.; Düssmann, H.; Sun, S.; Müller, B. J.; Prehn, J.; Baklaushev, V. P.; Klimant, I.; Papkovsky, D. B. Versatile Conjugated Polymer Nanoparticles for High-Resolution O_2 Imaging in Cells and 3d Tissue Models. *ACS Nano* **2015**, *9*, 5275−5288.
(37) Ho, L.-C.; Wu, W.-C.; Chang, C.-Y.; Hsieh, H.-H.; Lee, C.-H.; Chang, H.-T. Aptamer-Conjugated Polymeric Nanoparticles for the Detection of Cancer Cells through "Turn-on" Retro-Self-Quenched Fluorescence. *Anal. Chem.* **2015**, *87*, 4925−4932.
(38) Jia, Y.; Zuo, X.; Lou, X.; Miao, M.; Cheng, Y.; Min, X.; Li, X.; Xia, F. Rational Designed Bipolar, Conjugated Polymer-DNA Composite Beacon for the Sensitive Detection of Proteins and Ions. *Anal. Chem.* **2015**, *87*, 3890−3894.
(39) Sanromán-Iglesias, M.; Zhang, K. A.; Chuvilin, A.; Lawrie, C.; Grzelczak, M.; Liz-Marzan, L. M. Conjugated Polymers as Molecular Gates for Light-Controlled Release of Gold Nanoparticles. *ACS Appl. Mater. Interfaces* **2015**, *7*, 15692−15695.
(40) Wang, H.; Li, Y.; Chen, Y.; Li, L.; Fang, T.; Tang, Z. Development of a Conjugated Polymer-Based Fluorescent Probe for Selective Detection of Hocl. *J. Mater. Chem. C* **2015**, *3*, 5136−5140.
(41) Justice, J. B., Jr. Quantitative Microdialysis of Neurotransmitters. *J. Neurosci. Methods* **1993**, *48*, 263−276.
(42) Martin, A. R.; Vasseur, J. J.; Smietana, M. Boron and Nucleic Acid Chemistries: Merging the Best of Both Worlds. *Chem. Soc. Rev.* **2013**, *42*, 5684−713.
(43) Borisov, S. M.; Mayr, T.; Mistlberger, G.; Waich, K.; Koren, K.; Chojnacki, P.; Klimant, I. Precipitation as a Simple and Versatile Method for Preparation of Optical Nanochemosensors. *Talanta* **2009**, *79*, 1322−1330.
(44) Ahnert-Hilger, G.; Bräutigam, M.; Gratzl, M. Calcium-Stimulated Catecholamine Release From Alpha-Toxin-Permeabilized Pc12 Cells: Biochemical Evidence for Exocytosis and Its Modulation by Protein Kinase C and G Proteins. *Biochemistry* **1987**, *26*, 7842−7848.

DOI: 10.1021/acsami.5b04987
ACS Appl. Mater. Interfaces 2015, 7, 18581−18589